



First-principles calculation on dilute magnetic alloys in zinc blend crystal structure



Hamid Ullah ^{a,*}, Kalsoom Inayat ^a, S.A. Khan ^b, S. Mohammad ^b, A. Ali ^c, Z.A. Alahmed ^d, A.H. Reshak ^{e,f}

^a Department of Physics, Government Post Graduate Jahanzeb College, Saidu Sharif Swat, Pakistan

^b Department of Physics, Materials Modeling Laboratory, Hazara University, Mansehra 21300, Pakistan

^c Department of Advanced Materials Science & Engineering, Hanseo University, Seosan-si, Chungnam-do 356-706, Republic of Korea

^d Department of Physics and Astronomy, King Saud University, Riyadh 11451, Saudi Arabia

^e New Technologies-Research Center, University of West Bohemia, Univerzitni 8, 306 14 Pilsen, Czech Republic

^f Center of Excellence Geopolymer and Green Technology, School of Material Engineering, University Malaysia Perlis, 01007 Kangar, Perlis, Malaysia

ARTICLE INFO

Article history:

Received 26 November 2014

Received in revised form

10 February 2015

Accepted 27 February 2015

Available online 2 March 2015

Keywords:

Dilute magnetic semiconductor

Spintronic

Half metallicity

Density of states

ABSTRACT

Ab-initio calculations are performed to investigate the structural, electronic and magnetic properties of spin-polarized diluted magnetic alloys in zinc blende structure. The first-principles study is carried out on Mn doped III–V semiconductors. The calculated band structures, electronic properties and magnetic properties of $\text{Ga}_{1-x}\text{Mn}_x\text{X}$ ($\text{X}=\text{P}, \text{As}$) compounds reveal that $\text{Ga}_{0.75}\text{Mn}_{0.25}\text{P}$ is half metallic turned to be metallic with increasing x to 0.5 and 0.75, whereas substitute P by As cause to maintain the half-metallicity nature in both of $\text{Ga}_{0.75}\text{Mn}_{0.25}\text{As}$ and $\text{Ga}_{0.5}\text{Mn}_{0.5}\text{As}$ and tune $\text{Ga}_{0.25}\text{Mn}_{0.75}\text{As}$ to be metallic.

Calculated total magnetic moments and the robustness of half-metallicity of $\text{Ga}_{0.75}\text{Mn}_{0.25}\text{P}$, $\text{Ga}_{0.75}\text{Mn}_{0.25}\text{As}$ and $\text{Ga}_{0.5}\text{Mn}_{0.5}\text{As}$ with respect to the variation in lattice parameters are also discussed. The predicted theoretical evidence shows that some Mn-doped III–V semiconductors can be effectively used in spintronic devices.

© 2015 Published by Elsevier B.V.

1. Introduction

The III–V semiconductors and their alloys are extensively used in photonics and optoelectronics. These materials are mostly used for high-frequency light emitting diodes, optical detectors and laser diodes due to their high melting points, high thermal conductivity, large bulk modulus and wide band gaps. The binary compounds GaP and GaAs have been very promising candidates for advance technology. Most interestingly their band gap can be varied by alloying. This alloying effectively increases the range of applications of GaP and GaAs compounds [1–7].

Diluted magnetic semiconductors (DMS) are very promising materials for optoelectronic and spintronics applications. III–V compounds when doped with 3d transition elements this turn them to be as III–V DMS. The III–V DMS compounds attracted consideration for the possible increase in efficiency and miniaturization of the electronic devices [16]. Different DMS compounds [7–15] have been intensively studied theoretically as well as experimentally to design efficient devices like super smart diodes,

super smart memory chips, spin valves and spin field effect transistors. It is essential to explain the known properties of a given material designed for the fabrication of highly efficient electronic and spintronics devices and even to predict different properties of hypothetical materials.

For the analysis and calculation, computer modeling and simulation techniques are used as a consequence of the complication in the growth, characterization and procedure of these properties. The prediction of different properties of materials has been simplified by the use of modern technology and computational techniques with the first principle calculation. The computational techniques have already been applied to numerous materials with the first principle and predicted that theoretical results agree well with the experimental results.

In this article the structural, electronic and magnetic properties of $\text{Ga}_{1-x}\text{Mn}_x\text{P}$ and $\text{Ga}_{1-x}\text{Mn}_x\text{As}$ ($x=0.25, 0.50, 0.75$) alloys are studied by using density functional theory (DFT) within the state-of-the-art all-electron full potential linear augmented plane wave (FP-LAPW) method as implemented in WIEN2k code [17], which has proven to be one of the most accurate methods for the computation of the electronic structure of solids within DFT [18–21]. The ground state energy, optimum volume, bulk modulus, derivatives of the bulk modulus, band structures and density of states

* Corresponding author.

E-mail address: hamidullah@yahoo.com (H. Ullah).

are calculated and analyzed in details. The magnetic properties are predicted through the density of states analysis and magnetic moments.

2. Method of calculation

In the full-potential scheme, radial function, times waves function, potential and charge density are extended into two basis sets. Inside each atomic sphere the wave function is extended in spherical harmonics while in interstitial region it is extended to plane-wave basis. In similarly fashion the potential is extended as [22,23].

$$V(r) = \left\{ \sum_{lm} V_{lm}(r) Y_{lm}(\hat{r}) \right. \quad (1a)$$

$$V(r) = \left\{ \sum_K V_K e^{iKr} \right. \quad (1b)$$

Here Eq.1a is express the potential inside the sphere, whereas Eq.1b for the potential in the interstitial site. Inside the sphere the wave function is extended in terms of spherical harmonics up to $l_{\max}=9$. The potential is constant outside the sphere while spherically symmetric within the muffin-tin sphere. For the transition metal doped with III–V semiconductors the plane wave cut-off value of $K_{\max} * R_{MT}$ is chosen to be equal to 8. On the basis of convergence test, a mesh of 120 k -points and $G_{\max}=24$ are used for well converged results.

3. Results and discussions

3.1. Structural properties

To calculate the ground state properties of $\text{Ga}_{0.75}\text{Mn}_{0.25}\text{X}$, $\text{Ga}_{0.50}\text{Mn}_{0.50}\text{X}$ and $\text{Ga}_{0.25}\text{Mn}_{0.75}\text{X}$ ($\text{X}=\text{P}, \text{As}$), the volume of super cell was optimized by Birch Murnaghan's equation of state [23]. The optimization is also important to expose the magnetic nature of the alloys. The total energy as function of volume of the alloys is calculated for ferromagnetic and anti-ferromagnetic states. The total energy difference ($\Delta E = E_{\text{AFM}} - E_{\text{FM}}$) as listed in Table 1 show that the ferromagnetic states are more stable than that of anti-ferromagnetic states. The other structural parameters are also mentioned in the Table 1. At the optimized volume we have calculated the structural parameters such like the lattice constant a , bulk modulus B and derivative of the bulk modulus B^P within general gradient approximation (PBE-GGA) as shown in Table 1. Following Table 1, it is obvious that by increasing the concentration of Mn in GaP and GaAs the lattice constant decreases due

Table 1

Calculated lattice constant a_0 , Bulk Modulus B , Derivative of Bulk Modulus, B^P , and ground state ferromagnetic (FM) and anti-ferromagnetic (AFM) energies $\text{Ga}_{0.75}\text{Mn}_{0.25}\text{X}$, $\text{Ga}_{0.50}\text{Mn}_{0.50}\text{X}$ and $\text{Ga}_{0.25}\text{Mn}_{0.75}\text{X}$ ($\text{X}=\text{P}, \text{As}$).

Parameters	$\text{Ga}_{0.75}\text{Mn}_{0.25}\text{P/As}$	$\text{Ga}_{0.50}\text{Mn}_{0.50}\text{P/As}$	$\text{Ga}_{0.25}\text{Mn}_{0.75}\text{P/As}$
Lattice constant (Å)	5.49/5.69	5.45/ 5.73	5.42/5.71
Bulk modulus (GPa)	80.25/76.98	67.76/53.03	82.64/67.58
B^P	5.0/5.0	5.0/5.0	5.0/5.0
E_{FM} (Ry)	−16718.973818/ −32063.406665	−7566.529118/ −15249.934951	−13576.980958/ −28921.700885
E_{AFM} (Ry)	−16718.973814/ −32063.406663	−7566.529116/ −15249.934948	−13576.980954/ −28921.700882

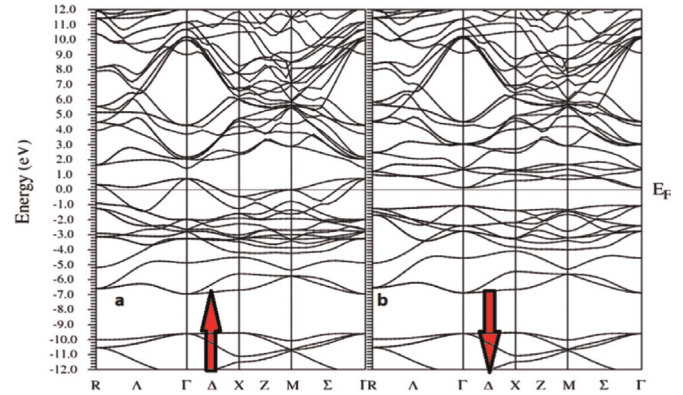


Fig. 1. Calculated band structure of $\text{Ga}_{0.75}\text{Mn}_{0.25}\text{P}$. (a) Spin (\uparrow) and (b) Spin (\downarrow).

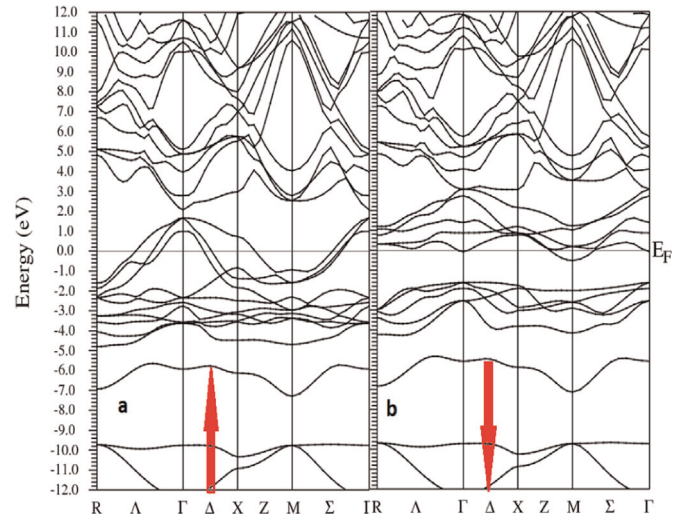


Fig. 2. Calculated band structure of $\text{Ga}_{0.50}\text{Mn}_{0.50}\text{P}$. (a) Spin (\uparrow) and (b) Spin (\downarrow).

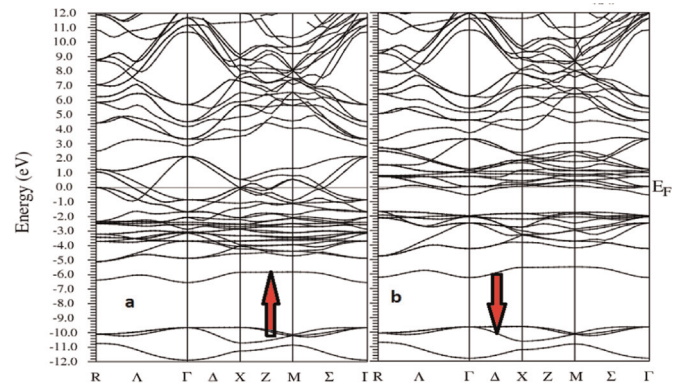


Fig. 3. Calculated band structure of $\text{Ga}_{0.25}\text{Mn}_{0.75}\text{P}$. (a) Spin (\uparrow) and (b) Spin (\downarrow).

the smaller volume of Mn than Ga. Similarly by substituting P by As the lattice constant also decreases due to the smaller volume of As than P. The spin polarized electronic band structures, magnetic properties and robustness of half-metallicity are further calculated by using the calculated lattice constants.

3.2. Band structure and density of states

The spin polarized electronic band structures in the first Brillouin zone are calculated along the symmetry directions for $\text{Ga}_{0.75}\text{Mn}_{0.25}\text{X}$, $\text{Ga}_{0.50}\text{Mn}_{0.50}\text{X}$ and $\text{Ga}_{0.25}\text{Mn}_{0.75}\text{X}$ ($\text{X}=\text{P}, \text{As}$), as prototype we show the electronic band structures of $\text{Ga}_{1-x}\text{Mn}_x\text{P}$

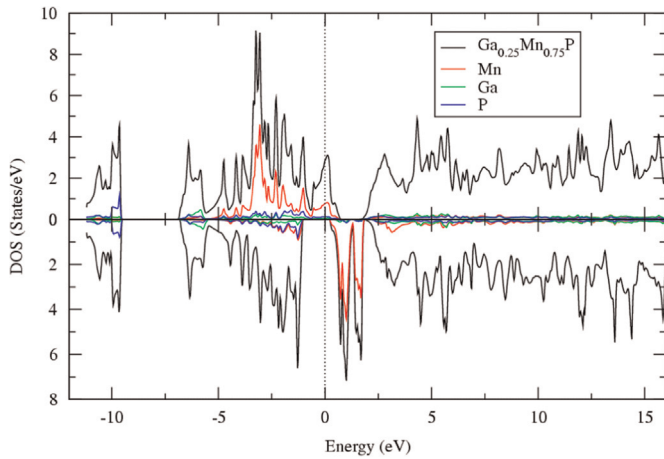


Fig. 4. Calculated total and partial density of states of $\text{Ga}_{0.75}\text{Mn}_{0.25}\text{P}$ for spin up and spin down.

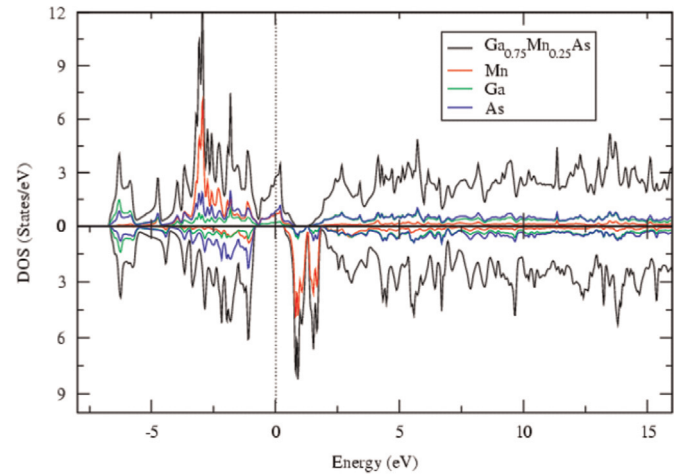


Fig. 7. Calculated total and partial density of states of $\text{Ga}_{0.75}\text{Mn}_{0.25}\text{As}$ for spin up and spin down.

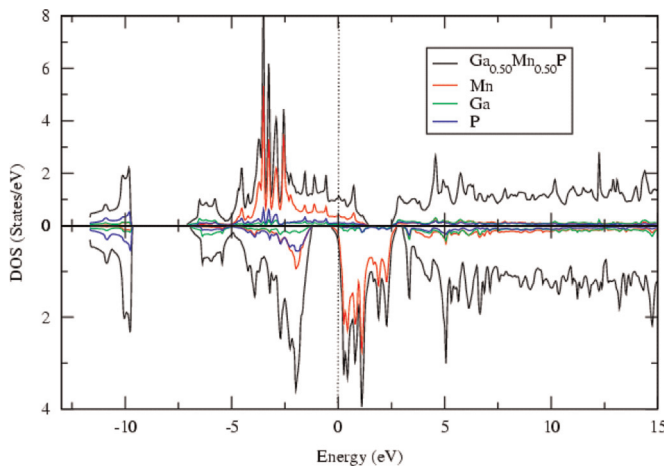


Fig. 5. Calculated total and partial density of states of $\text{Ga}_{0.50}\text{Mn}_{0.50}\text{P}$ for spin up and spin down.

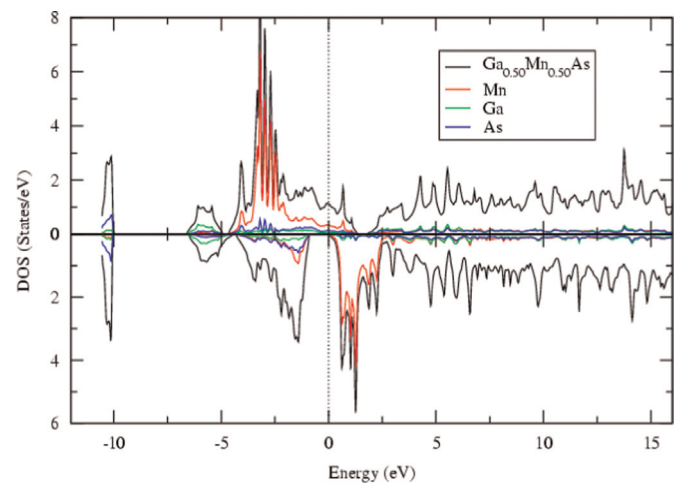


Fig. 8. Calculated total and partial density of states of $\text{Ga}_{0.50}\text{Mn}_{0.50}\text{As}$ for spin up and spin down.

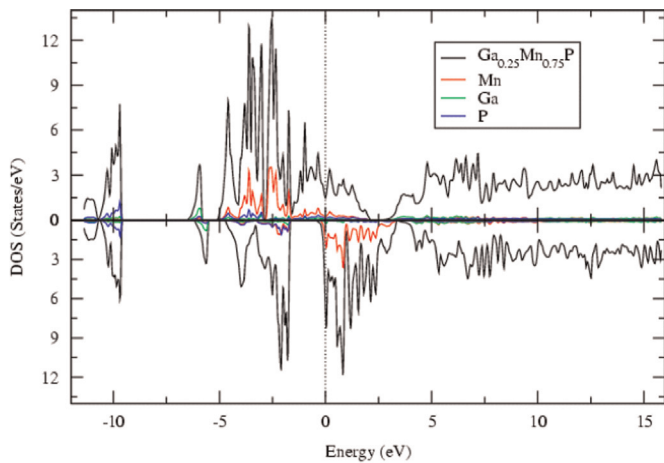


Fig. 6. Calculated total and partial density of states of $\text{Ga}_{0.25}\text{Mn}_{0.75}\text{P}$ for spin up and spin down.

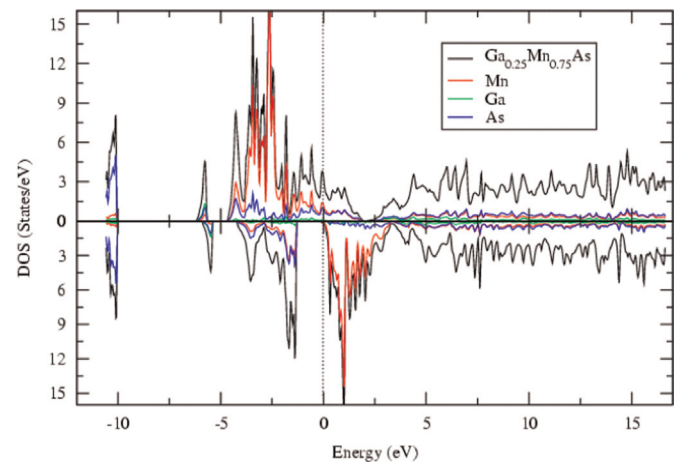


Fig. 9. Calculated total and partial density of states of $\text{Ga}_{0.25}\text{Mn}_{0.75}\text{As}$ for spin up and spin down.

as presented in Figs. 1–3. It is clear that the spin up (\uparrow) state contain more electrons than that of spin down (\downarrow) state. The results also exhibit that a band gap exists around the Fermi level for spin down state of $\text{Ga}_{0.75}\text{Mn}_{0.25}\text{P}$, $\text{Ga}_{0.75}\text{Mn}_{0.25}\text{As}$ and $\text{Ga}_{0.5}\text{Mn}_{0.5}\text{As}$ alloys, while for spin up state a few of the valence bands crosses the Fermi level and relocated to the conduction band, hence are

predicted to be half-metallic. A metallicity nature is observed in the $\text{Ga}_{0.5}\text{Mn}_{0.5}\text{P}$, $\text{Ga}_{0.25}\text{Mn}_{0.75}\text{P}$ and $\text{Ga}_{0.25}\text{Mn}_{0.75}\text{As}$ alloys for the spin up/dn. Based on this discussion one can conclude that increasing the x content in $\text{Ga}_{0.75}\text{Mn}_{0.25}\text{P}$ to 0.5 and 0.75 turn the compound to be metallic, whereas $\text{Ga}_{0.75}\text{Mn}_{0.25}\text{As}$ maintain the

Table 2
Calculated magnetic moments of Ga_{0.25}Mn_{0.75}X, Ga_{0.50}Mn_{0.50}X, Ga_{0.75}Mn_{0.25}X (X= P, As) in the zinc blended phase.

Material	$M^{\text{Int}} (\mu_B)$	$M^{\text{Mn}} (\mu_B)$	$M^{\text{Ga}} (\mu_B)$	$M^{\text{P}} (\mu_B)$	$M^{\text{As}} (\mu_B)$	$M^{\text{T}} (\mu_B)$
Ga _{0.75} Mn _{0.25} P	0.41405	3.61285	0.03203	-0.0306	-	4.00045
Ga _{0.50} Mn _{0.50} P	0.39427	3.52194	0.06612	-0.0419	-	3.89862
Ga _{0.25} Mn _{0.75} P	0.8005	3.44312	0.08581	-0.0908	-	10.8526
Ga _{0.75} Mn _{0.25} As	0.32683	3.74437	0.02977	-	-0.040	4.00055
Ga _{0.50} Mn _{0.50} As	0.27494	3.81485	0.06311	-	-0.0763	4.00025
Ga _{0.25} Mn _{0.75} As	0.78318	3.82311	0.09938	-	-0.1001	11.9517

half-metallicity nature with increasing the x content to 0.5 then turned to be metallic with further increasing in x content ($x=0.75$). The observed half-metallic in Ga_{0.75}Mn_{0.25}As agree well with that reported in Refs. [24,25]. For spin down state the Ga_{0.75}Mn_{0.25}P, Ga_{0.75}Mn_{0.25}As and Ga_{0.5}Mn_{0.5}As alloys are direct band gap semiconductors, the top of the valence and bottom of conduction bands occur at Γ symmetry point. The calculated band gap of Ga_{0.75}Mn_{0.25}P, Ga_{0.75}Mn_{0.25}As and Ga_{0.5}Mn_{0.5}As alloys are 1.2 eV, 1.4 eV and 1.6 eV, respectively. It can also be noted that by doping transition metal cause to decrease the band gaps to be lower than that of pure GaP ($E_g^{\Gamma-x} = 1.45$ eV) and GaAs ($E_g^{\Gamma-\Gamma} = 1.06$ eV) [26]. Transition from indirect to direct band gap in case of GaP appears to take place, which is optically active. In the presence of local strain and local electric field of Mn atom, a decrease in the band gaps is occur. The larger band gap Mn doped GaP can be related to the larger gap of pure GaP and GaAs.

With the aid of the partial density of states one can understand the origin of states/bands of Ga_{1-x}Mn_xX (X=P, As) as shown in Figs. 4–9. It is obvious from these figures that the bands in the locality of Fermi level are mostly due to Mn-3d state, X-p (X=P, As) states with small contribution from the Mn-4s state. The Fermi level is completely occupied for spin up state of Ga_{1-x}Mn_xX (X=P, As) alloys, while it is empty for the spin down state of Ga_{0.75}Mn_{0.25}P, Ga_{0.75}Mn_{0.25}As and Ga_{0.5}Mn_{0.5}As alloys. At the Fermi level the difference between spin up and spin down states causes 100% spin polarization [27]. The main cause of this spin polarization is spd-hybridization of Mn-3d, Mn-4s and X-p (X=P, As) states [28]. Hence the main cause of half-metallicity in TM doped GaP and GaAs is spd-hybridization. The partial occupancy for spin down state at the Fermi level is the basis of net magnetic moment in these compounds. The 5-fold degenerate Mn-3d state splits by the crystal field energy into doubly degenerate e_g -state and triply degenerate t_{2g} -state. The splitting is the result of the electric field generated by the p orbital of X (X=P, As) affecting Mn-3d states. The crystal field splitting energies can be calculated using the relation;

$$\Delta E_{\text{crystal}} = E_{t_{2g}} - E_{e_g}$$

Figs. 4–9, shows that t_{2g} state lie above e_g state, which shows that Mn is sitting in tetrahedral rather than octahedral crystal field atmosphere of GaP and GaAs lattice. These states shows that wave functions strongly hybridizes for t_{2g} state and weakly for e_g state with X-p (X=P, As) producing bonding and anti-bonding hybrids. Where, bonding and anti-bonding hybrids lie within the valence band and gap respectively. This hybrid shifts the valence band of the compound to higher energies. The more Mn doped GaP shows a stronger repulsion between bonding and anti-bonding than Mn doped GaAs, due to the fact that GaP has smaller ionicity and larger co-valency than GaAs.

3.3. Magnetic properties and robustness of half-metallicity

The calculated ground state ferromagnetic (FM) energy for each compound is less than the corresponding anti-ferromagnetic (AFM) energy as presented in Table 1. Hence on the basis of

ground state energies, we conclude that Ga_{0.75}Mn_{0.25}X, Ga_{0.50}Mn_{0.50}X and Ga_{0.25}Mn_{0.75}X (X=P, As) are ferromagnetic which is agree well with the previous finding that the ferromagnetism in these compounds have been reported experimentally [29–32]. GaMnP and GaMnAs exist in zinc blende structure [33]. They cannot be exactly described as a GaAs structure with all Ga substituted by Mn but some of Mn resides on interstitial sites [34,35]. The Mn-3d states is main source of the magnetization in Ga_{0.75}Mn_{0.25}X, Ga_{0.50}Mn_{0.50}X and Ga_{0.25}Mn_{0.75}X (X=P, As). While within the Mn-3d state the magnetic nature of the compounds may be related to partially filled t_{2g} states [27]. Table 2 shows the calculated total magnetic moments of the compounds and partial magnetic moments at interstitial and anti-sites. The magnetic moments at anti-sites (P and As) with negative values shows that the induce magnetic moments on these atoms are anti-parallel to Mn atoms and interact anti-ferromagnetically, While the positive values indicates parallel magnetic moment to Mn.

From the calculated density of states that P/As-s state and Mn-4s state repel each other. P/As-s is pushed towards core and Mn-4s towards Fermi level. The spd-hybridization is produced when Mn-s and Mn-4d states overlapped with P/As-p state. The local magnetic moment of Mn is reduced from its free space magnetic moment $4 \mu_B$ to a non integer value by spd-hybridization as given in Table 2, which clarifies that the net magnetic moment for all the studied compounds are whole number ($4 \mu_B$) which agree with Ref. [36]. The Ga_{0.75}Mn_{0.25}P, Ga_{0.75}Mn_{0.25}As and Ga_{0.5}Mn_{0.5}As alloys are half-metallic ferromagnet, which is evident from the integer magnetic moment ($4 \mu_B$) [37–40].

4. Conclusion

Mn doped III–V semiconductors were investigated with first principle calculations. The calculation reveals that Ga_{0.75}Mn_{0.25}P, Ga_{0.75}Mn_{0.25}As and Ga_{0.5}Mn_{0.5}As alloys are half-metallic and have direct band gap for spin down state. Whereas the Ga_{0.5}Mn_{0.5}P, Ga_{0.25}Mn_{0.75}P and Ga_{0.25}Mn_{0.75}As alloys are metallic for the spin up/dn. The results revealed that the ferromagnetic states are more stable than anti-ferromagnetic. The lattice constant is found to decrease by replacing Ga by Mn. It is also observed that spd-hybridization occur due to the spin channels and the electronic cloud of P/As-p states overlaps with the TM-3d and 2s states. We hope our findings may help for the development of different magneto electronic devices like HDI, ZIP, FeRAM etc.

Acknowledgments

The result was developed within the CENTEM project, reg. no. CZ.1.05/2.1.00/03.0088, cofunded by the ERDF as part of the Ministry of Education, Youth and Sports OP RDI programme and, in the follow-up sustainability stage, supported through CENTEM PLUS (LO1402) by financial means from the Ministry of Education, Youth and Sports under the "National Sustainability Programme I.

Computational resources were provided by MetaCentrum (LM2010005) and CERIT-SC (CZ.1.05/3.2.00/08.0144) infrastructures.

References

- [1] J. Zutic, Fabian, S.D. Sarma, *Rev. Mod. Phys.* 76 (2004) 323.
- [2] I.I. Mazin, *Appl. Phys. Lett.* 77 (2000) 3000.
- [3] T. Dietl, *J. Phys.: Condens. Matter* 19 (2007) 165204.
- [4] G. Burkard, G. Seelig, D. Loss, *Phys. Rev. B* 62 (1999) 2581.
- [5] G.A. Prinz, *Science* 282 (1998) 1660–1663.
- [6] H. Ohno, A. Shen, F. Matsukura, A. Oiwa, A. Endo, S. Katsumoto, Y. Iye, *Appl. Phys. Lett.* 69 (1996) 363.
- [7] B. Amin, Iftikhar Ahmad, M. Maqbool, S. Goumri-Said, R. Ahmad, *J. Appl. Phys.* 109 (2011) 023109.
- [8] B. Amin, I. Ahmad, M. Maqbool, *J. Light Wave Technol.* 28 (2010) 223.
- [9] S. Drablia, H. Meradji, S. Ghemid, S. Labidi, B. Bouhafs, *Phys. Scr.* 79 (2009) 045002.
- [10] Y.K. Kuo, B.T. Liou, S.H. Yen, H.Y. Chu, *Opt. Commun.* 237 (2004) 363–369.
- [11] R. de Paiva, J.L.A. Alves, R.A. Nogueira, C. de Oliveira, H.W.L. Alves, L.M. R. Scolfaro, J.R. Leite, *Mater. Sci. Eng. B* 93 (1–3) (2002) 2–5 30.
- [12] Y.A. Pusep, M.T.O. Silva, J.R.L. Fernandez, V.A. Chitta, J.R. Leite, T. Frey, D.J. As, D. Schikora, K. Lischka, Raman study of collective plasmon-longitudinal optical phonon excitation in cubic GaN and $\text{Al}_x\text{Ga}_{1-x}\text{N}$ epitaxial layer, *J. Appl. Phys.* 91 (2002) 6197–6199.
- [13] E. Martinez-Guerrero, E.B. Amalric, L. Martinet, G. Feuillet, B. Daudin, H. Mariette, P. Holliger, C. Dubois, C. Bru-Chevallier, P. Nze, T. AbougheChassagne, G. Ferro, Y. Monteil, Structural properties of undoped and doped cubic GaN grown on SiC(001), *J. Appl. Phys.* 91 (2002) 4983–4987.
- [14] E. Martinez-Guerrero, C. Adelman, F. Chabuel, J. Simon, N.T. Pelekanos, G. Mula, B. Daudin, G. Feuillet, H. Mariette, Self-assembled zinc blende GaN quantum dots grown by molecular beam epitaxy, *Appl. Phys. Lett.* 77 (2000) 809.
- [15] H. Okumura, H. Hamaguchi, T. Koizumi, K. Balakrishnan, Y. Ishida, M. Arita, S. Chichibu, H. Nakanishi, T. Nagatomo, S. Yoshida, Growth of cubic III-nitrides by gas source MBE using atomic nitrogen plasma: GaN, AlGaN and AlN, *J. Cryst. Growth* 390 (1998) 189–190.
- [16] C. Ronning, P.X. Gao, Y. Dind, Z.L. Wang, D. Schwen, *Appl. Phys. Lett.* 84 (2004) 783.
- [17] P. Blaha, K. Schwarz, G.K.H. Madsen, D. Kvasnicka, J. Luitz, WIEN2K—An Augmented Plane Wave & Local Orbital Program for Calculating Crystal Properties, Techn. Universitat, Wien, Austria, 2001, ISBN: 3-9501031-1-1-2.
- [18] Y. Saeed, S. Nazir, A. Shaukat, A.H. Reshak, *J. Magn. Magn. Mater.* 322 (2010) 3214–3222.
- [19] Mohammed Benali Kanoun, A.H. Reshak, Nawel Kanoun-Bouayed, Souraya Goumri-Said, *J. Magn. Magn. Mater.* 324 (2012) 1397–1405.
- [20] Hardev S. Saini, Mukhtiyar Singh, A.H. Reshak, ManishK. Kashyap, *J. Magn. Magn. Mater.* 331 (2013) 1–6.
- [21] A.H. Reshak, Z. Charifi, H. Baaziz, *J. Magn. Magn. Mater.* 326 (2013) 210–216.
- [22] S. Me^c-abih, K. Benguerine, N. Benosman, B. Abbar, B. Bouhafs, *Physica B* 403 (2008) 3452.
- [23] F. Birch, Finite elastic strain of cubic crystals, *Phys. Rev.* 71 (1947) 809–824.
- [24] E. Kulatov, H. Nakayama, H. Mariette, H. Ohta, Y.A. Uspenskii, Electronic structure, magnetic ordering, and optical properties of GaN and GaAs doped with Mn, *Phys. Rev. B* 66 (2002) 045203.
- [25] L.M. Sandratskii, P. Bruno, J. Kudrnovsky, On-site Coulomb interaction and the magnetism of (GaMn)N and (GaMn)As, *Phys. Rev. B* 69 (2004) 195203.
- [26] D. Khanin, S. Kulkova, *Russ. Phys. J.* 48 (2005) 70.
- [27] B. Amin, I. Amad, Theoretical investigation of half metallicity in Fe/Co/Ni doped ZnSe material systems, *J. Appl. Phys.* 106 (2009) 093710.
- [28] R. de Paiva, R.A. Nogueira, Electronic structure and magnetic properties of $\text{Al}_{1-x}\text{Mn}_x\text{N}$ alloys, *J. Appl. Phys.* 96 (2004) 6565.
- [29] M. Kaminska, A. Twardowski, D. Wasik, Mn and other magnetic impurities in GaN and other III–V semiconductors – perspective for spintronics application, *J. Mater. Sci. Mater. Electron.* 19 (2008) 828–834.
- [30] S.J. Pearton, M.E. Overberg, G.T. Thaler, C.R. Abernathy, J. Kim, F. Ren, N. Theodoropoulou, A.F. Hebard, Y.D. Park, Room temperature ferromagnetism in GaMnN and GaMnP, *Phys. Status Solidi A* 195 (2003) 222–227.
- [31] M.E. Overberg, K.H. Baik, G.T. Thaler, C.R. Abernathy, S.J. Perton, J. Kelly, R. Rairigh, A.F. Hebard, W. Tang, M. Stavola, J.M. Zavada, *Electrochem. Solid-state Lett.* 6 (2003) 131.
- [32] H. Kato, K. Hamaya, T. Taniyama, Y. Kitamoto, H. Munekata, Ion irradiation control of ferromagnetism in (Ga,Mn)As, *Jpn. J. Appl. Phys.* 44 (2005) 816–818.
- [33] F. Glas, G. Patriarche, L. Largeau, A. Lemaître, Determination of the local concentrations of Mn interstitials and antisite defects in GaMnAs, *Phys. Rev. Lett.* 93 (2004) 086107.
- [34] K.M. Yu, W. Walukiewicz, T. Wojtowicz, I. Kuryliszyn, X. Liu, Y. Sasaki, J. K. Furdyna, Effect of the location of Mn sites in ferromagnetic $\text{Ga}_{1-x}\text{Mn}_x\text{As}$ on its Curie temperature, *Phys. Rev. B* 65 (2002) 201303.
- [35] J. Mašek, J. Kudrnovsky, F. Maca, *Phys. Rev. B* 67 (2003) 153203.
- [36] T. Ogawa, M. Shirai, N. Suzuki, I. Kitagawa, First-principles calculations of electronic structures of diluted magnetic semiconductors (Ga,Mn)As, *J. Magn. Magn. Mater.* 196 (1999) 428–429.
- [37] G.Y. Gao, K.L. Yao, E. Sasioglu, L.M. Sandratskii, Z.L. Liu, J.L. Jiang, Half-metallic ferromagnetism in zinc-blende CaC, SrC, and BaC from first principles, *Phys. Rev. B* 75 (2007) 174442.
- [38] L. Adamowicz, M. Wierzbicki, Symmetry induced half-metallic alkaline earth ferromagnetic, *Acta Phys. Pol. A* 115 (2009) 217.
- [39] M. Zhang, E. Bruk, F.R.D. Boer, G. Wu, Half-metallic ferromagnetism in hypothetical wurtzite MBi ($M=V, Cr, Mn$), *J. Appl. Phys.* 97 (2005) 10C306.
- [40] Z. Wu, R.E. Cohen, *Phys. Rev. B* 73 (2006) 235116.